TAM receptors and the regulation of erythropoiesis in mice

Hongmei Tang,[1] Song Chen,[1] Haikun Wang,[1] Hui Wu,[1] Qingxian Lu,[2] and Daishu Han[1]

[1]Department of Cell Biology, Institute of Basic Medical Sciences, Chinese Academy of Medical Sciences, School of Basic Medicine, Peking Union Medical College, Beijing; [2]Department of Ophthalmology, School of Medicine, Capital Medical University, Beijing, China

Citation: Tang H, Chen S, Wang H, Wu H, Lu Q, and Han D. TAM receptors and the regulation of erythropoiesis in mice. Haematologica 2009; doi:10.3324/haematol.13635

Supplementary methods

Reverse transcriptase polymerase chain reaction

Total RNA was extracted using TRIzol™ reagent (Invitrogen, Carlsbad, CA, USA) according to the manufacturer's instructions. Expression of Tyro3, Axl, and Mer was examined by reverse transcriptase (RT) polymerase chain reaction (PCR) with cycles of 94°C for 30 seconds, annealing at appropriate temperature based on primer pairs for 30 seconds and extension at 72°C for 45 seconds. The number of PCR cycles corresponded to a range in which a linear increase in products could be detected. β-actin was used as a control. Real-time PCR were performed to analyze expression of EpoR, Epo, GATA-1, GATA-2, STAT1, STAT3 and STAT5a with the power SYBR® Green PCR master mix kit (Applied Biosytems, Forster City, CA, USA) using an ABI PRISM 7300 real-time cycler (Applied Biosytems). The transcript level of target genes was normalized to GAPDH. The sequences of primer pairs for the PCR are listed in *Online Supplementary Table S1*.

Immunocytochemistry staining

The erythroid cells were cytospun onto poly-L-lysine–coated slides, air dried and fixed with 4% paraformaldehyde solution (pH 7.4) for 20 minutes at room temperature. Endogenous peroxidase of the cells was inactivated by treatment with 3% hydrogen peroxide for 15 minutes at room temperature. The cells were incubated with normal blocking serum at room temperature for 30 minites to reduce non-specific binding. Goat anti-mouse Tyro3, Axl and Mer polyclonal antibodies (Santa Cruz Biotechnology, Santa Cruz, CA, USA) were applied overnight at 4°C in a moist chamber. The cells were then incubated with horseradish peroxidase/Fab polymer conjugated rabbit anti-goat IgG (Zhongshan, Beijing, China) at room temperature for 30 minutes. Peroxidase activity was visualized with diaminobenzidine. Pre-immune goat sera were used as the first antibody in negative controls.

Western blotting

Cells were lysed with lysis buffer containing 1 mU/mL aprotinin, 0.1 mM leupeptin and 0.5 mM PMSF, and the supernatant was separated by 10% SDS-PAGE and subsequently electrotransferred onto PVDF membranes (Millipore, Bedford, MA, USA). After blocking with 2% BSA in PBS containing 0.1% Tween-20 (PBS-T) for 1 hour, the membranes were incubated with the primary polyclonal antibodies against Tyro 3, Axl, and Mer at 4°C overnight. The membranes were then incubated with horseradish peroxidase-conjugated rabbit anti-goat IgG (Zhongshan) at room temperature for 1 hour. Antigen-antibody complexes were visualized using an enhanced chemiluminescence detection kit (Zhongshan).

Online Supplementary Table S1. Primer sets used for polymerase chain reactions.

	Gene	Primer pairs (5'→3', Forward and Reverse)	T_m (°C)	Size (bp)
	β-actin	CCATCACCATCTTCCAGGAG CCTGCTTCACCACCTTCTTG	55	445
	Axl	AGGCTCATTGGCGTCTGTT ATCGCTCTTGCTGGTGTAG	54	399
RT-PCR	Mer	CCTGGTTTTGATGGCTACTC GGAGGCTTCGTCCATCTAAT	54	311
	Tyro3	TGAAGCCCGCAACATAAA TCCCATTCCAGGATAAGG	55	420
	Gapdh	CAACGGGAAGCCCATCAC CGGCCTCACCCCATTTG	58	65
	EpoR	AGTGAGCATGCCCAGGACA AAGTCAGACGGGCAGGAAGAT	59	149
	Epo	CATCTGCGACAGTCGAGTTCTG TGCACAACCCATCGTGACAT	59	76
Real-time RT-PCR	GATA-1	CAAGAAGCGTTTGATTGTCAG AGTGTTGTGGTGGTCGTTTG	60	71
	GATA-2	CAAGGATGGCGTCAAGTACCA TCCATCTTCATGCTCTCGGAG	60	51
	STAT1	CGGAGTCGGAGGCCCTAAT ACAGCAGGTGCTTCTTAATGAG	62	140
	STAT3	CAATACCATTGACCTGCCGAT GAGCGACTCAAACTGCCCT	62	109
	STAT5a	TGCCATTGACTTGGACAATCC AAACCCATCTTCCCCCACC	59	112
	Wild-type	AGAAGGGGTTAGATGAGGAC		
Genotyping	Axl	GCCGAGGTATAGTCTGTCACAG	53	368
	Mutant	AGAAGGGGTTAGATGAGG		
	Axl	TTTGCCAAGTTCTAATTCCATC	53	200

Phagocytosis of senescent red blood cells by peritoneal macrophages

Resident peritoneal macrophages were collected from mouse peritoneal cavities by lavage with 5 mL cold PBS containing 2% fetal calf serum (FCS), and cultured in Dulbecco's modified Eagle's medium (DMEM) supplemented with 10% FCS in a humidified incubator with 5% CO_2 at 37°C. The red blood cells (RBC) were isolated from peripheral blood and exposed to 3 mM phenylhydrazine (Sigma) in PBS for 1 hour at 37°C, which induces a translocation of phosphatidylserine from the inner to the outer membrane surface. Cells were then labeled using 10 μg/mL FITC (Sigma) in PBS for 30 minutes at 37°C. After three washes with PBS, the FITC-conjugated RBC were resuspended in DMEM and co-cultured with the macrophages for 30 minutes at 37°C with 5% CO_2. The cultures were washed three times with PBS, and RBC that had not been engulfed were removed by incubating in the lysis buffer for 10 seconds. The cells were examined under a microscope (X71, Olympus).

Supplementary results

Impaired erythropoiesis in Axl$^{-/-}$Mer$^{-/-}$ mice

During analysis of the phenotypes of mice mutant for TAM receptors, we found that the bone marrows of adult mice doubly mutant for Axl and Mer (Axl$^{-/-}$Mer$^{-/-}$) were pale compared to those of wild-type controls (*Online Supplementary Figure S1A*). This phenotype was not observed in mice singly mutant for Axl (Axl$^{-/-}$) or Mer (Mer$^{-/-}$). Histological analysis showed that the sinusoids in wild-type bone marrows were filled with red cells, whereas those in the Axl$^{-/-}$Mer$^{-/-}$ bone marrows were largely empty and contained fewer red cells (*Online Supplementary Figure S1B*). The histological appearance of the bone marrows of Axl$^{-/-}$ or Mer$^{-/-}$ single mutant mice was similar to that of the wild-type controls. To analyze the cellularity of the bone marrows further, total bone marrow cells from adult mice (10 weeks old) were counted with a hemacytometer (*Online Supplementary Figure S1C*). We found that the bone marrow of Axl$^{-/-}$Mer$^{-/-}$ mice contained fewer cells than that of the wild-type controls ($1.6\pm0.04\times10^7$ *vs.* $2.7\pm0.06\times10^7$/femur, $n = 8$, $p<0.01$). By flow cytometry, we found that Axl$^{-/-}$Mer$^{-/-}$ bone marrow contained fewer nucleated erythroblasts (Ter119+) than bone marrow from wild-type controls ($0.4\pm0.02\times10^7$ *vs.* $0.7\pm0.03\times10^7$/femur, n=6, $p<0.01$). Mature red cells were decreased by 2.7-fold in Axl$^{-/-}$Mer$^{-/-}$ bone marrow (0.3± 0.01_107 *vs.* $0.8\pm0.02\times10^7$/femur, n=8, $p<0.01$). In contrast, the bone marrow cellularity in single mutant mice (Axl$^{-/-}$ or Mer$^{-/-}$) was not significantly different from that of wild-type controls (*Online Supplementary Figure S1C*).

Impaired bone marrow erythropoiesis may result in anemia in Axl$^{-/-}$Mer$^{-/-}$ mice. We, therefore, analyzed hematologic parameters of the mice at different ages. Peripheral blood (50 μL) was collected from a bleeding tail vein into an Eppendorf tube containing 50 μL of 10 mM EDTA in PBS. Hematologic measurements were performed on an ADVIA 2120 Hematology Analyzer (Bayer Diagnostics, German). Unexpectedly, we found comparable hematologic parameters

Online Supplementary Table 2. BFU-E and CFU-E in bone marrow and spleen.

Source	Wild-type	Axl$^{-/-}$Mer$^{-/-}$
Bone marrow		
Erythroid cells (×10^6/femur)	15.7 ± 0.8	7.4 ± 0.3*
BFU-E (×10^3/femur)	15.2 ± 0.5	17.0 ± 1.0
CFU-E (×10^4/femur)	16.4 ± 0.4	29.6 ± 1.3*
Spleen		
Erythroid cells (×10^6/spleen)	30.5 ± 1.2	198.1 ± 7.9**
BFU-E (×10^3/spleen)	3.1 ± 0.2	96.5 ± 5.7**
CFU-E (×10^4/spleen)	7.6 ± 0.2	790.5 ± 48.2**

Single-cell suspensions were isolated from the bone marrows and spleens of mice (10 weeks old). The number of BFU-E and CFU-E was determined by clonogenic assays. Erythroid cell numbers were estimated by flow cytometry. The data are mean ± SEM of five individual mice. (*) p<0.05, (**) p<0.01.

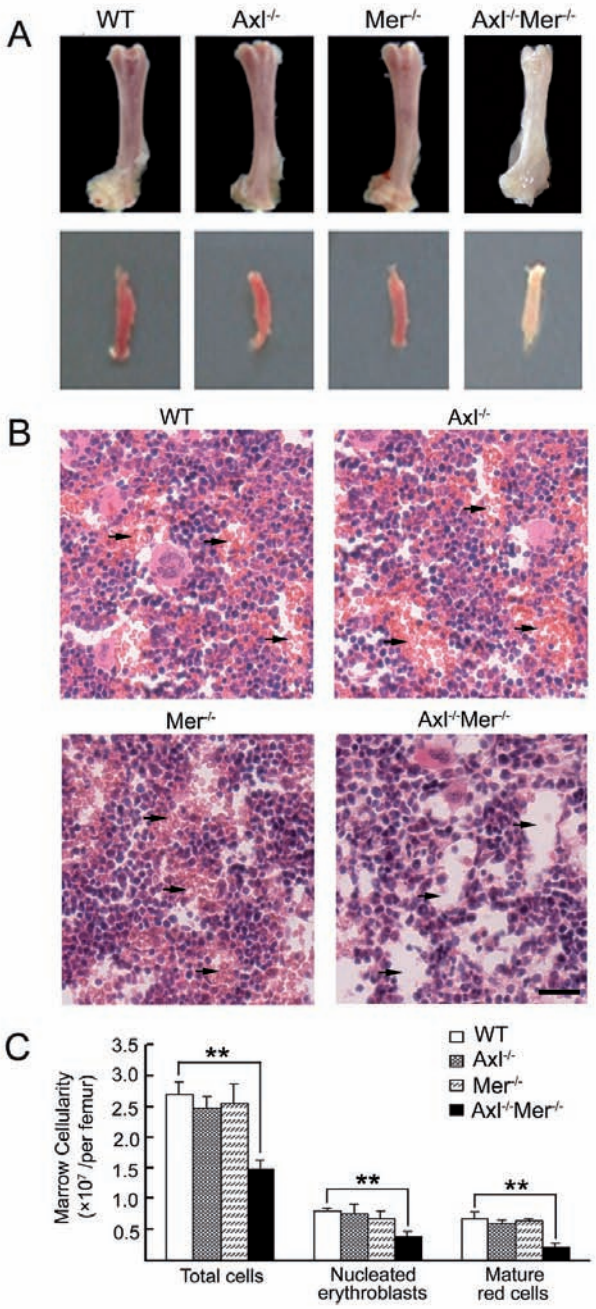

Online Supplementary Figure S1. Reduction of erythroid cells in Axl$^{-/-}$Mer$^{-/-}$ bone marrow. (A) Femora and bone marrows from adult mice. Axl$^{-/-}$Mer$^{-/-}$ mice had markedly pale bone marrow. (B) Representative hematoxylin and eosin-stained sections of the bone marrows viewed at 200× magnification showing the sinusoids (arrows), which are filled with mature red cells in wild-type (WT) bone marrow, but largely empty in Axl$^{-/-}$Mer$^{-/-}$ bone marrow. Scale bar = 20 μm. (C) The bone marrow cellularity of the respective genotypically different mice. The data are the mean ± SEM of five mice of each genotype, (**) $p<0.01$. All the analyses were performed with bone marrow from 10-week old mice.

between Axl$^{-/-}$Mer$^{-/-}$ mice and wild-type controls up to 15 months old (*data not shown*). Furthermore, based on Giemsa staining and cytometric analysis, we did not find morphologically abnormal RBC or CD11b^{+}Gr-1^{+} immature myloid cells in the peripheral blood of Axl$^{-/-}$Mer$^{-/-}$ mice. These observations may suggest that a compensatory extramedullary erythropoiesis occurs in Axl$^{-/-}$Mer$^{-/-}$ mice. In this study, we found that the weight of Axl$^{-/-}$Mer$^{-/-}$ spleens is increased by up to 4 times that of wild-type controls in 10-week old mice (*Online Supplementary Figures S2A, B*). Histological examination of the enlarged spleens showed an evident expansion of red pulp and invasion of the red pulp into white pulp (*Online Supplementary Figure S2C*, upper panel). The sinusoids of spleens from Axl$^{-/-}$Mer-$^{-/-}$ mice were dramatically enlarged and filled with abundant red cells, indicating active splenic erythropoiesis (*Online Supplementary Figure S2C*, lower panel). By contrast, the sinusoids in spleens from wild-type mice contained fewer red cells compared to the Axl$^{-/-}$Mer$^{-/-}$ spleens. The total spleen cells were increased by 4 times in Axl$^{-/-}$Mer$^{-/-}$ mice compared to wild-type controls (*Online Supplementary Figure S2D*). Spleens from Axl$^{-/-}$Mer$^{-/-}$ mice had about 17.2-fold increased nucleated erythroblasts and 10.8-fold increased mature red cells compared to spleens from wild-type controls (*Online Supplementary Figure S2D*). The expanded splenic erythropoiesis in Axl$^{-/-}$Mer$^{-/-}$ mice could compensate the impaired bone marrow erythropoiesis to maintain normal numbers of peripheral RBC. To analyze the expression of TAM receptors in splenic erythroblasts, we isolated Ter119+ cells from wild-type and Axl$^{-/-}$Mer$^{-/-}$ spleens and performed RT-PCR using RNA from the cells. We did not find signals for any of the three receptors in Axl$^{-/-}$Mer$^{-/-}$ splenic erythroid cells (*data not shown*), whereas Axl and Mer, but not Tyro3, were detected in wild-type splenic Ter119^{+} cells (*Online Supplementary Figure S2E*). Therefore, Tyro3 could not be involved in the expanded splenic erythropoiesis in Axl$^{-/-}$Mer$^{-/-}$ mice.

It has been shown that loss of Mer results in impaired phagocytosis of apoptotic cells by macrophages. The steady numbers of circulating RBC may be also, at least in part, attributable to a reduced rate of clearance of senescent RBC in Axl$^{-/-}$

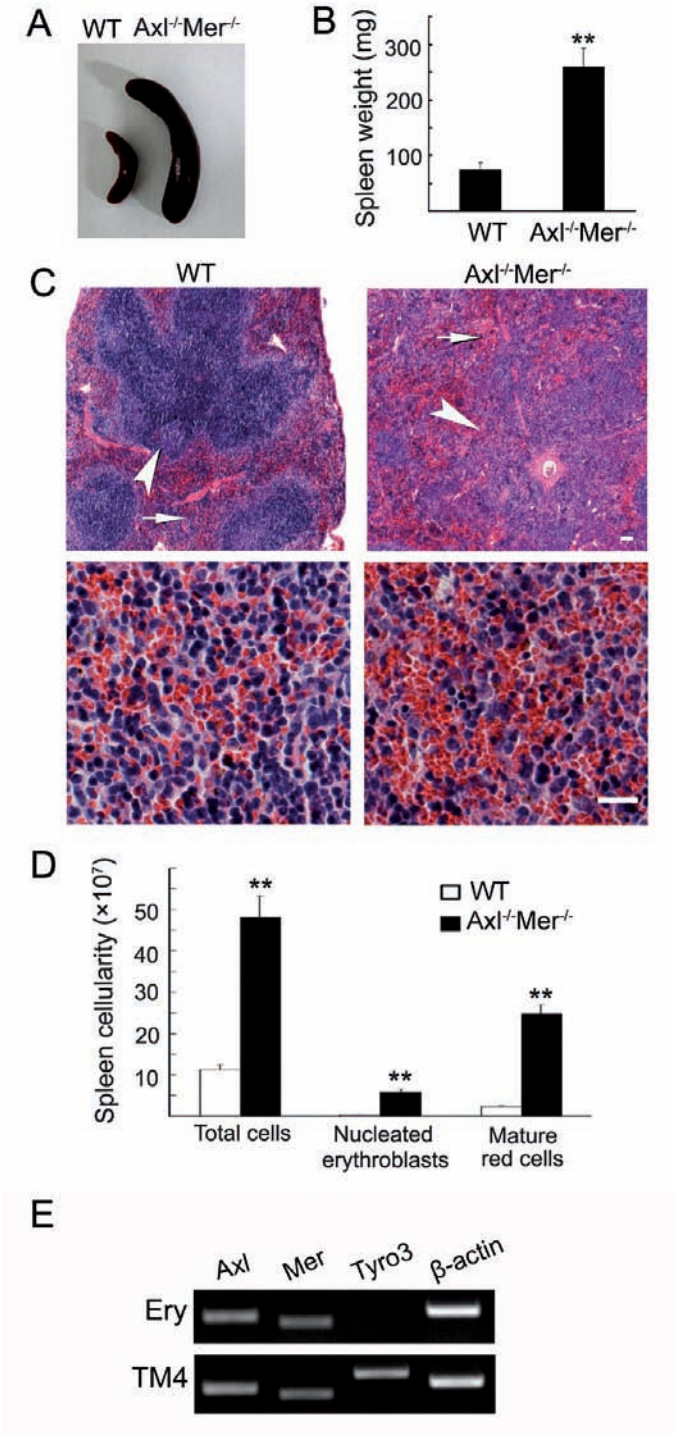

Online Supplementary Figure S2. Expanded splenic erythropoiesis in Axl$^{-/-}$Mer$^{-/-}$ mice. (A) Representative spleens of wild-type (WT) littermates and Axl$^{-/-}$Mer$^{-/-}$ mice at the age of 10 weeks. (B) The weight of spleens. The data are mean ± SEM of ten mice, (**) p<0.01. (C) Representative hematoxylin and easin-stained sections of WT and Axl$^{-/-}$Mer$^{-/-}$ spleens. The upper panels were viewed at 100× magnification, showing white pulp (arrowheads) and red pulp (arrows). The lower panels were amplifications (400×) of red pulp, showing expanded sinusoids in Axl$^{-/-}$Mer$^{-/-}$ spleen. Scale bar = 20 μm. (D) Cellularities of WT and Axl$^{-/-}$Mer$^{-/-}$ spleens (n = 5). (E) Expression of TAM receptors in splenic erythroblasts. Tyro3 mRNA was not detected in splenic erythroblasts by RT-PCR (upper panel). TM4 cells were used as controls (lower panel), and β-actin was used to monitor the quality of samples.

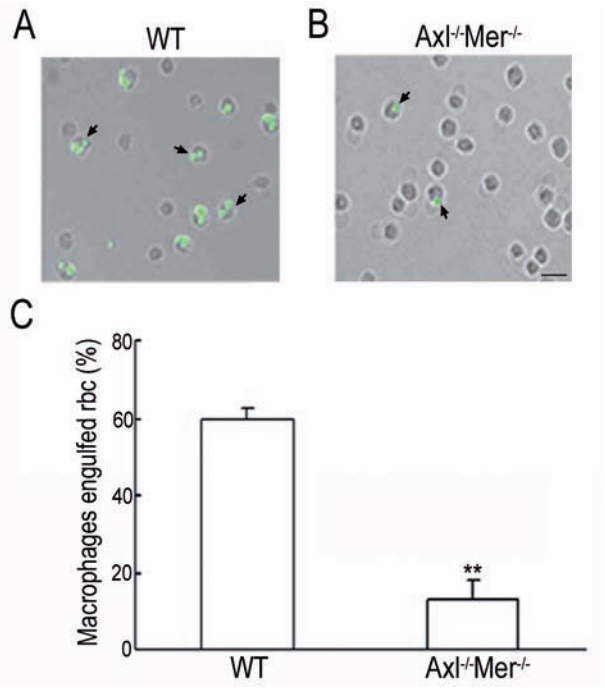

Online Supplementary Figure S3. Phagocytosis of senescent RBC by macrophages. (A) Wild-type (WT) peritoneal macrophages containing engulfed FITC-labelled RBC (arrows). (B) Axl$^{-/-}$Mer$^{-/-}$ peritoneal macrophages containing engulfed FITC-labelled RBC (arrows). (C) Quantification of the macrophages with internalized RBC. The data are mean ± SEM (n = 200), (**) p<0.01.

$Mer^{-/-}$ mice. To examine this possibility, we performed phagocytosis assays to evaluate the clearance rate of phenylhydrazine-treated RBC by peritoneal macrophages. The results showed that the number of macophages that engulfed senescent RBC was reduced by about 5-fold in $Axl^{-/-}Mer^{-/-}$ mice (*Online Supplementary Figure S3*). This reduction in engulfment of senescent RBC by macrophages could decrease the clearance rate of the senescent cells, and result in a prolongation of RBC survival in $Axl^{-/-}Mer^{-/-}$ mice. To examine the *in vivo* life span of RBC, the cells were biotinylated *in vivo* by an intravenous infusion of NHS-biotin (Invitrogen) as previously described.[1] Senescent RBC were detected by flow cytometry 30 days after biotinylation as the cells labeled with both biotin and FITC-conjugated annexin V. The results showed a higher percentage of circulating senescent RBC in $Axl^{-/-}Mer^{-/-}$ mice than in wild-type mice (0.29%±0.05% *vs.* 0.15%±0.02%, n=6, $p<0.05$). These data indicate that RBC in $Axl^{-/-}Mer^{-/-}$ mice have a longer lifespan because senescent RBC are not efficiently cleared.

References

1. Dale GL, Daniels RB, Beckman J, Norenberg SL. Characterization of senescent red cells from the rabbit. Adv Exp Med Biol 1991;307:93-103.